ORIGINAL ARTICLE

Evaluation of Ovarian Radiation Dose from Internally Scattered X-rays in Posteroanterior (PA) Chest Radiography With and Without Contact Gonad Shielding: Phantom Study

Siti Nur Atiqah Mat lazin[1], Inayatullah Shah Sayed[1,*]

[1]Department of Diagnostic Imaging and Radiotherapy, Kulliyyah of Allied Health Sciences, International Islamic University Malaysia, 25200 Kuantan, Pahang, Malaysia

Keywords:
internally scattered radiation; ovarian dose; ESD; contact shielding; radaition protection

ABSTRACT

Background: Scattered radiation originating from the patient's body disperses unevenly in multiple directions, posing a risk of incidental exposure to radiosensitive organs, such as the ovaries, which may absorb radiation from internally scattered X-rays. Although external radiation shielding is a common practice, internal scatter from within the patient presents additional complexities. This study aimed to quantify the radiation dose received by the ovaries using optically stimulated luminescence dosimeters (OSLDs) in posteroanterior (PA) chest X-ray examinations, both with and without the application of a contact gonad shield. **Methods:** A Siemens Multix Top X-ray imaging system was utilized for this study, operating with tube voltages between 70 kVp and 100 kVp and employing Automatic Exposure Control (AEC). The source-to-image distance (SID) was consistently maintained at 180 cm. The entrance skin dose (ESD) measurements corresponding to the ovaries were conducted using nanoDot OSLDs. These were positioned within the RANDO phantom at slice 29 to align with the anatomical location of the ovaries. Measurements taken with and without the use of a contact gonad shield. **Results:** The recorded ovarian ESD with contact gonad shielding averaged 2.2, 2.4, 3.7, and 3.0 mGy at 70, 80, 90, and 100 kVp, respectively. In contrast, without contact gonad shielding, the average ovarian ESD observed at 1.0, 1.8, 2.6, and 3.1 mGy at the respective tube voltages. Radiation dose (ESD) by each ovary varied based on the kVp and the use of contact gonad shielding. Results indicated an unexpected increase in ovarian dose with the use of a contact gonad shield, and a consistent rise in ESD noted with increasing kVp, irrespective of shielding. **Conclusion:** Scatter radiation in radiography presents a risk to organs beyond the primary imaging area, particularly the ovaries in posteroanterior (PA) chest radiography. Research indicates that higher tube potentials result in increased ESD to the ovaries. Interestingly, contact gonad shielding, a conventional method to reduce exposure, may not significantly lower radiation exposures and could potentially increase dose to ovaries. Therefore, discontinuing contact gonad shields seems justifiable for radiation safety. Optimization of tube voltage and tight collimation are crucial for minimizing ovarian radiation exposure.

INTRODUCTION

The chest X-ray is among the most commonly performed radiological examinations, serving as a primary diagnostic tool to guide further diagnosis, treatment, and follow-up (Sun et al., 2012). Although the radiation dose for each examination is relatively low, the widespread use of chest X-rays contributes to a significant collective dose. Skinner (2015) emphasized that chest radiography is an essential starting point in imaging, offering comprehensive views of the lungs and cardiovascular system through standard posteroanterior (PA) and lateral projections, enhancing patient management and quality of life. However, careful attention to radiation dose is essential. Although the lifetime cancer risk from chest radiography is low, implementing dose-reduction strategies remains critical. Bontrager et al., (2024) highlighted the importance of tailoring projections (PA, AP, or lateral) to fit the patient's anatomy, clinical indications, and safety requirements. Radiation safety in diagnostic radiography includes minimizing patient exposure through collimation, lead shielding, and optimized technical settings to maintain image quality without increasing the dose. Shielding against backscatter radiation is equally important, ensuring that the benefits of radiography outweigh the risks.

The scatter radiation, also known as secondary radiation, disperses in all directions after interacting with body tissues, posing an unnecessary exposure risk to both patients and healthcare staff (Insight Medical Imaging, 2019). Ahmed & Shaddad (2002) reported that scatter

* *Corresponding author.*
E-mail address: inayatullah@iium.edu.my

Journal homepage: https://journals.iium.edu.my/ijahs/index.php/IJAHS
EISSN NO 2600-8491

radiation occurs when the primary beam interacts with collimators, beam stops, or shielding. An enlarged field size also increases scatter radiation, potentially elevating the patient's radiation dose and diminishing image quality.

The amount of scatter radiation produced is influenced by the object imaged and the exposure settings. High-kVp techniques, frequently used in chest radiography, achieve uniform radiographic density and clearer visualization of lung markings. However, increased kVp also raises scatter radiation, which reduces image contrast. Using a grid suited to the selected tube potential can help minimize scatter radiation. Naji et al., (2017) observed that as kVp exceeds 70, photon penetration increases, but image contrast diminishes. Higher kVp also elevates Compton scattering probability, increasing the scatter-to-primary ratio up to 120 kVp, after which it stabilizes (Ghafarian et al., 2007).

The "As Low as Reasonably Achievable" (ALARA) principle is foundational in radiography, guiding practitioners to minimize radiation doses without compromising diagnostic quality (ICRP, 2007). This principle emphasizes weighing the benefits and risks of radiation exposure and ensuring each exposure is justified by evaluating factors such as body part, examination type, radiation dose, and technical settings (IAEA, 2002). Chest radiography, though involving a relatively low dose, is the most frequent radiological procedure, accounting for 43% of plain radiography cases (Ministry of Health Malaysia, 2009). Its routine use across large patient numbers necessitates that technologists adhere to the ALARA principle, ensuring high-quality imaging with minimal radiation exposure.

Protecting patients of childbearing age from radiation is especially important, as ionizing radiation can have severe biological impacts on radiosensitive tissues like the ovaries (Goodman & Amurao, 2012). Prior research has underscored the need to estimate ovarian doses during PA chest radiography. Ionizing radiation in routine exams like chest radiography is a significant concern, given its daily clinical use and cumulative contribution to the collective effective dose (Matyagin & Collins, 2016). Scatter radiation impacts both radiation safety and image quality. Jaenisch et al., (2010) explained that scatter radiation from X-ray photon interactions affects image clarity and contributes to patient and clinician dose (Abrantes et al., 2017; Lima, 2009). Maddox (2019) noted that scattering results in deflected radiation that travels in various directions, leading to exposure of organs outside the primary imaging area, such as the ovaries. Gonad shielding has traditionally been used to reduce radiation exposure to the ovaries, yet recent studies suggest internal scattered radiation may still reach them.

The absorbed dose quantifies the energy absorbed per unit mass of tissue, assessing potential organ damage from radiation (Andisco, et al., 2014). Goodman & Amurao (2012) explained that ionizing radiation affects biological tissues by displacing electrons from atoms, which can damage cells, produce free radicals, and alter tissue structure. These effects are particularly severe in radiosensitive cells, such as those in ovarian or breast tissue.

This study investigates the etrance skin dose (ESD) to the ovaries during PA chest radiography at different tube potentails. Additionally, it assesses the effectiveness of contact gonad shielding in reducing ovarian exposure. The findings aim to offer valuable insights for future practices, especially implementing effective radiation protection measures.

MATERIALS AND METHODS

In this study, the RANDO phantom, illustrated in Figure 1, was used to simulate a patient for estimating the ESD to the ovaries in PA chest radiography. The phantom is horizontally sectioned into 2.5 cm thick slices, each numbered sequentially for easy identification. It contains holes that can be filled with bone-equivalent, soft-tissue-equivalent, and lung-tissue-equivalent inserts, as described by Tazehmahalleh et al., (2008).

Figure 1: RANDO Phantom used in this study

Fung & Gilboy (2001) identified that the ovarian site corresponds to slice 29 of the RANDO phantom. They further indicated that this location aligns with the iliac spine level, medially positioned relative to the vertical plane, within the true pelvis against the lateral wall.

For this study, a nanoDot OSL dosimeter from Nagase Landauer, Japan, was used (Figure 2). This dosimeter has a minimum detection threshold of approximately 0.1 mGy. It is designed for multiple uses post-exposure to X-rays,

with only a minor sensitivity loss of 0.04% over repeated readouts (Graeper, 2015). Al-Senan & Hatab (2011) reported that OSLDs exhibit excellent homogeneity (<5%) and reproducibility (3.3%), with a linear response.

Figure 2: nanoDot OSLD

The Landauer Microstar Reader (Figure 3) was employed for reading the nanoDot OSL dosimeter. This device operates with inLight Microstar Reader Software (version 5.0) and measures radiation doses by exciting the dosimeter with laser light. Once read, the data is extracted, analyzed, and stored. The reader allows for various calibration and configuration settings; however, it is limited to processing one dosimeter at a time. Pre-irradiation readings of nanoDot OSLDs were recorded to subtract from post-irradiation readings, ensuring accurate dose measurements.

Figure 3: The Landaeur MicroStar OSLD Reader

The data were collected by positioning the RANDO phantom in the posterior-anterior (PA) position. The phantom was placed upright on the table, facing the erect bucky, to simulate standard positioning for a chest X-ray examination. A 35 x 43 cm image receptor was inserted lengthwise inside the erect bucky. The source-to-image distance (SID) was fixed at 180 cm. The imaging parameters used in this study are shown in Table 1. A nanoDot OSLD was placed at the 29th slice of the phantom, identified as the location of the ovaries on both the right and left sides as shown in Figure 4. This placement is based on previous studies and research cited in Bardo et al., 2009.

The x-ray beam was tightly collimated to cover the entire lung region. The experiment then proceeded with the application of contact gonad shield to the phantom during the PA chest radiography. The setup of the RANDO phantom is shown in Figure 5.

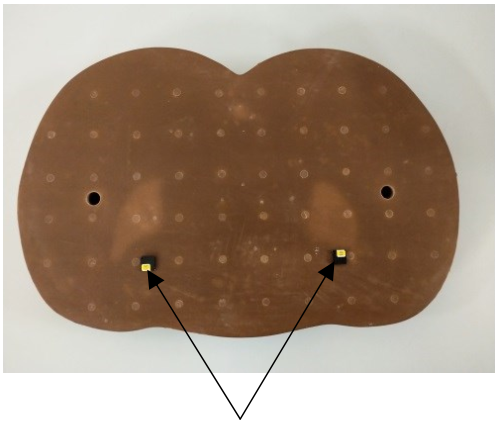

Figure 4: Placement of the nanoDot OSLDs at the 29th slice of the phantom

Table 1: The imaging parameters used in this study

PARAMETERS	DETAILS
Kilovoltage (kVp)	70, 80, 90, 100
Automatic Exposure Control (AEC)	On
Imaging plate size (cm), orientation	35 x 43, lengthwise
Central ray	Perpendicular to the center of IR, midsagittal plane at the level of T7
Source-to-image distance (cm)	180
Focal spot	Broad focal spot (1.0 mm)
Grid (grid ratio)	Moving grid (12:1)
Location of gonad shield	Inferior to iliac crest, 1 inch below the lower costal margin

Figure 5: RANDO phantom positioned PA erect against the erect bucky

The tube potential range for a PA chest x-ray projection varies from 55 to 125 kVp, with an exposure range of 2 to 30 mAs (Ng et al., 1998). Another study by Kim et al., (2007) reported a tube potential range of 54-150 kVp and an exposure range of 18-60 mAs. However, variations in exposure selection are often necessary to account for differences in patient body habitus, weight, and imaging requirements, with the goal of producing high-quality images while minimizing dose.

Statistical Analysis

The data for this study analyzed using IBM's Statistical Package for Social Sciences (SPSS), version 25. The Spearman's correlation test was employed to examine the relationship between the differences in ESD to the ovary during chest X-ray radiography, both with and without contact gonad shielding. The significance was performed at $p < 0.05$.

RESULT

Measured ESD to the Ovaries

ESD measurements corresponding to the ovaries were conducted using a RANDO phantom and nanoDot OSLD with and without contact gonad shielding to determine the effectiveness of gonadal shielding in PA chest radiography. Different tube potentials (with AEC on) were selected.

When using the gonad shield, the ESD to the ovaries showed inconsistencies between the right and left ovary. The ESD was slightly different for the right and left ovaries depending on the tube potential. With 80 kVp, 90 kVp, and 100 kVp, the right ovary received a higher dose than the left; however, at 70 kVp, the left ovary received a higher dose (0.0016 mGy) than the right ovary (0.0006 mGy). On average, the ESD for the right ovary increased at 70 kVp and 90 kVp, then decreased slightly at 100 kVp. The left ovary's ESD showed a fluctuating pattern, as illustrated in Figure 6. The highest ESD for the right ovary was 0.0022 mGy at 90 kVp, while the lowest for the left ovary was 0.0004 mGy at 80 kVp.

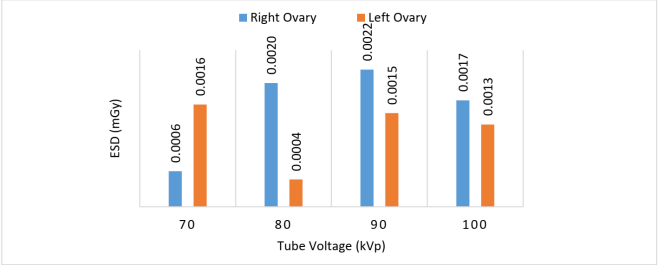

Figure 6: Measured ESD of right and left ovary with different tube potentials (with contact gonad shield)

In contrast, without gonad shielding, the ESD at 70 kVp was undetectable for the right ovary, while the left ovary absorbed a small dose of 0.0010 mGy. As the tube potential increased, the ESD to the right ovary also increased. The left ovary's dose increased up to 90 kVp and then sharply decreased to 0.0001 mGy at 100 kVp. The ESD trends for the right and left ovaries are shown in Figure 7.

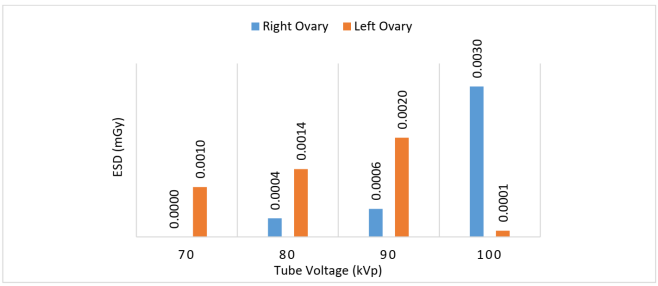

Figure 7: Measured ESD the right and left ovary at different tube potentials (without contact gonad shield)

The left ovary generally received a higher dose than the right, except at 100 kVp, where the highest dose of 0.0030 mGy was recorded. The lowest reading (no ESD) measured at 70 kVp.

The average ovarian ESDs with and without contact gonad shielding is shown in Figure 8. Overall, the total ESD to the ovaries with contact gonad shielding was higher than without it.

Correlation of ESD to the Ovaries and Tube Potential With and Without Contact Gonad Shield

In clinical practice, using contact gonad shielding during PA chest radiography is not a routine. This study primarily ovaries and varying tube potentials, with and without contact gonad shielding.

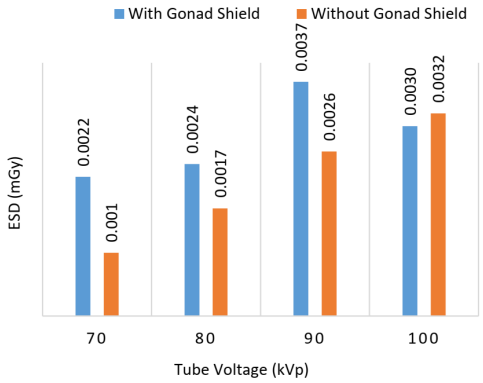

Figure 8: Average ESD to ovaries at different tube potentials with and without contact gonad shield

A bivariate Spearman's correlation test in SPSS was performed, revealing no significant difference between the absorbed dose to the ovaries and tube voltage with or without contact gonad shielding. The p-values were 0.247 (with shield) and 0.299 (without shield), both exceeding the significance level ($p > 0.05$) at a 95% confidence interval. Thus, using contact gonad shielding did not significantly affect the ESD to the ovaries or the tube exposure setting in PA chest radiography.

DISCUSSION

The study investigated the effects of ESD on the ovaries at different tube potentials during PA chest radiography, comparing results with and without the use of contact gonad shielding. No significant differences were observed in the ESD at different tube potentials, with and without the contact gonad shield.

During radiography, X-rays interact with the patient's body, resulting in internal scattering of radiation. This scattered radiation can be absorbed by tissues or organs beyond the targeted projection area, potentially increasing the risk of cancer due to unnecessary radiation exposure. Furthermore, the energy of scattered photons is unevenly distributed and radiates in all directions (Rehn, 2015). An illustration of internally scattered radiation within the phantom is shown in Figure 9.

Even though the ovaries lie outside the collimation area in PA chest radiography, however, still receive a dose from internal scatter. The results show that both the right and left ovaries are exposed to radiation, with variations in the ESD depending on tube potential and ovarian side. This aligns with the observation that scattered radiation disperses in all directions and is unevenly distributed.

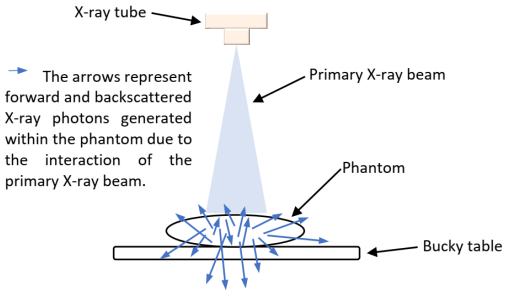

Figure 9: Illustration of internally scattered X-rays within the phantom

Effect of Different Tube Potentials on ESD to Ovaries With and Without Contact Gonad Shield

The highest recorded total ESD to both ovaries was 0.0037 mGy with contact gonad shield, which is still below 0.01 mGy as indicated in previous studies (Ogundare et al., 2009; Njeh et al., 1997). Figures 6 and 7 show that the ESD to the ovaries increases with higher tube potentials (kVp), as greater kVp enhances the X-ray beam's penetrating power and increases scatter radiation (Naji et al., 2017; Ghafarian et al., 2007). Notably, scatter radiation appears to increase with tube potentials up to 120 kVp and then slightly decrease at higher potentials. Thus, a high kVp technique in PA chest radiography may reduce the absorbed dose to the ovaries.

This study used tube potentials between 70 kVp and 100 kVp, selected based on prior research (Ng et al., 1998; Kim et al., 2006). Statistical analysis indicated no significant difference in ESDs to the ovaries across these tube potentials, our findings are consistent with previous research by Rosenstein (1988), which showed that increased kVp results in a higher dose to the ovaries.

Interestingly, the study found that ESD to the ovaries was higher with contact gonad shielding than without, as illustrated in Figures 6, 7 and 8. This contradicts the traditional practice of using contact gonad shields to reduce radiation dose. It suggests that internal scatter radiation generated within the phantom's body during exposure reached to the ovaries, regardless of contact gonad shielding. As Hiles et al., (2020) noted that internal scatter radiation within the patient is challenging to quantify but represents a significant source of secondary radiation exposure to organs outside the primary beam. Shielding one part of the body from another part internally is difficult, as shielding does not effectively reduce radiation dose at greater depths from the primary beam (<17 cm) (Hiles et al., 2020).

Ovaries Dose Differences With and Without Cotact Gonad Shielding

Statistical analysis revealed no significant difference in the ESD to the ovaries across various tube potentials with and without contact gonad shielding. This indicates that gonad shielding minimally affects ESD to the ovaries. Matyagin & Collins (2016) found that gonad shields in PA chest radiography provide only a small reduction in dose to deep-seated organs while slightly increasing skin dose due to scatter from the shield's internal surface. This means that scatter radiation from shielding may reflect back towards the patient. Hiles et al. (2020) also reported that gonad shielding does not significantly reduce dose outside the collimated area, further supporting this study's findings.

According to the American Association of Physicists in Medicine (AAPM, 2019), shielding does little to reduce patient exposure since any potential dose reduction is negligible compared to internal scatter radiation within the patient. Based on current evidence, the use of patient contact shielding is generally unnecessary and not recommended in diagnostic and interventional radiology. This study shows that contact gonad shielding can inadvertently increase patient dose by interfering with automatic dose control or necessitating repeat imaging if image quality is compromised. Effective positioning and optimized protocol parameters are more impactful for dose reduction than using gonad shields (Hiles et al., 2020).

Limitations of the Study

This study has several limitations. Using a RANDO phantom instead of real patients may not fully represent clinical conditions due to body habitus variations. Additionally, minimal ovarian dose from scatter radiation introduced variability in measurements, necessitating multiple measurements for accuracy. Sensitivity and proper application of nanoDot detectors also posed challenges in the experimental setup.

CONCLUSION

This study concludes that increasing tube potential correlates with higher ovarian doses, though contact gonad shielding does not significantly reduce this exposure. In fact, at 90 kVp, ovarian dose was highest with shielding, suggesting shielding may not enhance radiation safety. Therefore, optimizing tube potential and collimation is essential to uphold the ALARA (As Low As Reasonably Achievable) principle for radiation safety. In summary, internal scatter radiation poses a risk to organs outside the primary imaging area, particularly the ovaries in PA chest radiography. Since contact gonad shielding does not consistently reduce ESDs — and may even increase ovarian dose — its routine use appears unnecessary. Focusing on tube voltage optimization and precise collimation offers a more effective approach to minimizing ovarian radiation exposure.

Future Recommendations

For future research, it is recommended to explore a broader range of exposure settings with more than five tube potentials, repeated at least three times for greater accuracy. Additional sensitive organs, such as the thyroid and eyes, could be included in further studies. Additionally, using thermoluminescent dosimeters (TLDs) may offer improved sensitivity for measuring absorbed dose.

ACKNOWLEDGEMENT

The authors express their gratitude to the Department of Diagnostic Imaging and Radiotherapy, Kulliyyah of Allied Health Sciences, International Islamic University Malaysia, Kuantan Campus, for providing facilities and support necessary to conduct the experiments for this research. The staff's cooperation and technical assistance are greatly appreciated. This research received no funding.

REFERENCES

Abrantes, A., Rebelo, C., Sousa, P., Rodrigues, S., Almeida, R., Pinheir, J., Azevedo, K., Riberio, L. (2017). Scatter Radiation Exposure During Mobile X-Ray Examinations. *HealthManagement.org*, 17:68–72. https://healthmanagement.org/uploads/article_attachment/hm-v17-i1-abrantes-scatterradiation.pdf

Ahmed, A. A., & Shaddad, A. (2002). Measurement of Dose Received By Patients from Scattered Radiation in Diagnostic Radiology in Khartoum. *IAEA*, 35:557–568. http://www.iaea.org/inis/collection/NCLCollectionStore/ _Public/35/095/35095220.pdf

Al-Senan, R. M., & Hatab, M. R. (2011). Characteristics of an OSLD in the diagnostic energy range. *Medical Physics*, 38:4396–4405. https://doi.org/10.1118/1.3602456

American Association of Physicists in Medicine. (2019). Patient Gonadal and Fetal Shielding in Diagnostic Imaging Frequently Asked Questions. https://www.aapm.org/org/policies/documents/CA

RES_FAQs_Patient_Shielding.pdf

Andisco, D., Blanco, S., & Buzzi, A. E. (2014). Dosimetry in Radiology. *Radioprotection*, 78:114–117. http://www.webcir.org/revistavirtual/articulos/septiembre14/argentina/arg_ing_a.pdf

Bardo, D. M. E., Black, M., Schenk, K., & Zaritzky, M. F. (2009). Location of the ovaries in girls from newborn to 18 years of age: Reconsidering ovarian shielding. *Pediatric Radiology*, 39:253–259. https://doi.org/10.1007/s00247-008-1094-4

Bontrager, L. Kenneth, & Lampignano, J. (2024). *Textbook of radiographic positioning and related anatomy* (11th ed.). St. Louis: Mosby/Elsevier.

Fung, K. K. L., & Gilboy, W. B. (2001). The effect of beam tube potential variation on gonad dose to patients during chest radiography investigated using high sensitivity LiF: Mg, Cu, P thermoluminescent dosemeters. *The British Journal of Radiology*, 74:358–367. http://www.birpublications.org/doi/abs/10.1259/bjr.74.880.740358#.V_oRJgrAZw0.mendeley

Ghafarian, P., Ay, M. R., Ghadiri, H., Sarkar, S., & Zaidi, H. (2007). Impact of X-ray Tube Voltage, Field Size and Object Thickness on Scattered Radiation Distribution in Diagnostic Radiology: A Monte Carlo Investigation. *IEEE Nuclear Science Symposium Conference Record*, 3830–3834. https://www.hug.ch/sites/interhug/files/structures/pinlab/documents/MIC07_M19-191.pdf

Goodman, T. R., & Amurao, M. (2012). Medical Imaging Radiation Safety for the Female Patient: Rationale and Implementation. *RadioGraphics*, 32:1829–1837. doi: 10.1148/rg.326125508

Graeper, G. (2015). Efficacy of Reusing NanoDot OSL Dosimeters Using Optical Bleaching, Master Thesis, Oregon State University. http://hdl.handle.net/1957/56306

Hiles, P., Benson, E., Hughes, H., Loader, R., Shaw, D., Edyvean, S., et al. (2020, March). Guidance on using shielding on patients for diagnostic radiology applications. The British nstitute of radiology. https://www.bir.org.uk/media/414334/final_patient_shielding_guidance.pdf

IAEA. (2002). Radiological Protection of Patients In General Diagnostic Radiology (Radiography), 1–4. https://www-pub.iaea.org/MTCD/publications/PDF/csp_007c/PDF.../CSPS-7-P-CD.pdf

ICRP. (2007). The 2007 Recommendations of the International Commission on Radiological Protection. *ICRP Publication 103*, 37:2–4. http://www.icrp.org/publication.asp?id=ICRP Publication 103

Insight Medical Imaging. (2019, November 26). Scatter Radiation; Protecting our Staff & Patients. https://x-ray.ca/daily-insight/scatter-radiation-protection/.

Jaenisch, G. R., Ewert, U., & Jechow, M. (2010). Scatter Radiation in Radiography. 10th European Conference on Non-Destructive Testing, Moscow 2010, June 7-11. https://www.ndt.net/?id=9121

Kim, Y., Choi, J., Kim, C., Kim, J., Kim, S., Oh, Y., … Kim, C. (2007). Patient dose measurements in diagnostic radiology procedures in Korea. *Radiation Protection Dosimetry*, 123:540–545. https://doi.org/10.1093/rpd/ncl501

Lima , JJ (2009). *Techniques for diagnosis with X-ray - Physical Aspects and Biophysical (2nd ed.).* University of Coimbra

Maddox, M. (2019, April 11). What is Scatter Radiation? https://www.instadose.com/blog/what-is-scatter-radiation

Matyagin, Y. V, & Collins, P. J. (2016). Effectiveness of abnominal shields in chest rdiography- a monte carlo evaluation. *British Journal of Radiology*. 89:20160465. https://doi.org/10.1259/bjr.20160465

Ministry of Health Malaysia. (2009). Report of Medical Radiation Exposure Study in Malaysia. https://doi.org/10.1017/CBO9781107415324.004

Naji, A. T., Jaafar, M. S., Ali, E. A., & Al-Ani, S. K. J. (2017). Effect of Backscattered Radiation on X-Ray Image Contrast. *Applied Physics Research*, 9:105. https://doi.org/10.5539/apr.v9n1p105

Ng, K. H., Rassiah, P., Wang, H. B., Hambali, A. S., Muthuvellu, P., & Lee, H. P. (1998). Doses to patients in routine X-ray examinations in Malaysia. *The British Journal of Radiology*, 71:654–660. doi: 10.1259/bjr.71.846.9849390

Njeh, C. F., Wade, J. P., & Goldstone, K. E. (1997). The Use

of Lead Aprons in Chest Radiography. *Radiography*, 3: 143–147. https://www.sciencedirect.com/science/article/pii/S1078817497900195

Ogundare, F. O., Olarinoye, I. O., & Obed, R. I. (2009). Estimation of patients' organ doses and conceptus doses from selected X-ray examinations in two Nigeria X-ray centres. *Radiation Protection Dosimetry*, 132:395–402. https://doi.org/10.1093/rpd/ncn317

Rehn, E. (2015, June 24). Modeling of scatter radiation during interventional X-ray procedures. https://www.diva-portal.org/smash/get/diva2:826933/FULLTEXT01.pdf

Rosenstein, M. (1988). *HANDBOOK of Selected Tissue Doses for Projections Comman In Diagnostic Radiology*. https://www.fda.gov/media/74806/download

Skinner, S. (2015). Guide to thoracic imaging*, Australian Family Physician,* 44:558–563. https://www.racgp.org.au/afp/2015/august/guide-to-thoracic-imaging/

Sun, Z., Lin, C., Tyan, Y. S., & Ng, K.-H. (2012). Optimization of chest radiographic imaging parameters: a comparison of image quality and entrance skin dose for digital chest radiography systems. *PubMed*, 36:279–286. doi: 10.1016/j.clinimag.2011.09.006

Tazehmahalleh, F. E., Gholamhosseinian, H., Layegh, M., Tazehmahalleh, N. E., & Esmaily, H. (2008). Determining rectal dose through cervical cancer radiotherapy by 9 MV photon beam using TLD and XR type T GAFCHROMIC® Film. *Iran. J. Radiat. Res*, 6:129–134. http://ijrr.com/files/site1/user_files_fad21f/admin-A-10-1-289-bf100c3.pdf